Limitations of time-delayed case isolation in heterogeneous SIR models

Jonas Hansson, Alain Govaert, Richard Pates, Emma Tegling, Kristian Soltesz

***Abstract*— Case isolation, that is, detection and isolation of infected individuals in order to prevent spread, is a strategy to curb infectious disease epidemics. Here, we study the efficiency of a case isolation strategy subject to time delays in terms of its ability to stabilize the epidemic spread in heterogeneous contact networks. For an SIR epidemic model, we characterize the stability boundary analytically and show how it depends on the time delay between infection and isolation as well as the heterogeneity of the inter-individual contact network, quantified by the variance in contact rates. We show that network heterogeneity accounts for a restricting correction factor to previously derived stability results for homogeneous SIR models (with uniform contact rates), which are therefore too optimistic on the relevant time scales. We illustrate the results and the underlying mechanisms through insightful numerical examples.**

I. Introduction

A. Background

Early in an epidemic of a previously unknown infectious disease, transmitted through an unknown pathogen, existing pharmaceutical treatments may not be applicable or efficient. This was for example the case with COVID-19, caused by the pathogen SARS-CoV-2. In early 2020, countries across the world experienced exponential increases in detected SARS-CoV cases, hospitalizations, and ICU admittance due to COVID-19, and ultimately related deaths. While statistics are still debated one year later [1], it stood clear early on that pharmaceutical treatment and clinical care would not alone suffice to curb the epidemic outbreak.

The exponential increase of cases early in the epidemic prompts the implementation of schemes to reduce the number of probable transmission events. Such schemes are often referred to as non-pharmaceutical interventions (NPIs for short), and can be partitioned into two categories:

- Recommendations or legislation aimed at decreasing inter-individual contact rates;
- Schemes for case isolation through testing, and possibly contact tracing.

The former includes, for example, discouraging unnecessary in-person interaction, banning large gatherings, closing schools, or imposing societal lockdowns. The effectiveness of such interventions is still poorly understood. In particular, it can be practically challenging or impossible to estimate the effect of individual NPIs, particularly in the early transient phase of an epidemic, as demonstrated in [2], [3].

In light of the above, case isolation schemes have gained attention. In contrast to NPIs aimed at reducing contact rates in general, case isolation schemes target contacts involving infectious individuals. If successfully implemented, they could be the key to an open society where lockdowns are replaced by regular testing. Under such schemes, a positive test result leads to case isolation. The effectiveness of the scheme can be increased by complementing systematic testing with contact tracing.

It is intuitively evident that a case isolation scheme needs to identify and isolate positive cases in a timely manner in order to be effective. In [4], a comprehensive analysis was done, from a control-theoretic standpoint, of the performance and stability of case isolation schemes. We refer to references therein for relevant works in the epidemiology literature. There, as in our current work, one central question is that of time delays: how long can delays between infection and isolation be if we are to prevent epidemic outbreaks?

In this paper we investigate how the structure of social networks affect the effectiveness of case isolation schemes. This is done by deriving an explicit stability condition, which relates effectiveness to network heterogeneity. We use a simple epidemiological model; an SIR model for the early phases of an epidemic. This modeling choice is motivated by its sufficiency for the purpose of our analysis, and the lack of data to support high-complexity modeling.

B. Preliminaries

We consider a closed population. This is an optimistic approximation, since there will be no imported cases within the model. The population is partitioned into susceptibles, infectious and removed (recovered and permanently immune or deceased) proportions. Here, we will not distinguish between being infected and being infectious. However, the results we are about to present can easily be extended to cater for this distinction.

If the proportion of infectious goes to zero, the strategy has been successful. The question we consider is how large the infectious proportion can grow, relative to the susceptible, in order for a case isolation strategy to remain effective.

To answer this, we consider the setting early in an epidemic, where the proportion of susceptibles is much larger than the infectious and removed, respectively. This allows us to disregard herd immunity effects. Another way to put it is that in an interaction between two individuals where one is infectious, the other is susceptible (with probability one).

The authors are with the Department of Automatic Control, Lund University, Lund, Sweden. Email: {jonas.hansson, alain.govaert, richard.pates, emma.tegling, kristian.soltesz}@control.lth.se

This work was partially funded by the Swedish Research Council (grants 2017-04989, 2019-00691) and by the Wallenberg AI, Autonomous Systems and Software Program (WASP) funded by the Knut and Alice Wallenberg Foundation. The authors are members of the ELLIIT Strategic Research Area at Lund University.

Furthermore, we realistically assume the considered time window for our model to be short compared to the typical duration of immunity. This means that we neglect any flow from the removed to the susceptible sub-population. As with distinguishing between infected and infectious individuals, introducing such reflux dynamics into the model we propose is straightforward, should the considered disease differ in this aspect from SARS-CoV-2.

We will focus on criteria for stabilization of the early epidemic trajectory. We will refer to a case isolation scheme as stabilizing if it eventually empties the infectious sub-population. In the linearized model, this is done without decreasing the pool of susceptibles (in other words without the help of the herd immunity effect [5]), and in this sense, the stability criteria we derive are conservative.

Note that this stability condition does not specify *performance* in the sense that it may allow for a large infectious sub-population in the transient during which the infectious sub-population grows (due to the time delay before isolation) and empties. As such, this stability condition constitutes a bare minimum. Any practically feasible strategy would need to fulfill it with some performance margin, as further elaborated in [4].

Finally, we need to formalize our case isolation scheme. Here we will utilize a simple yet versatile model that quantifies the proportion of those infected on a given day that is subsequently isolated by the scheme T_{delay} days later. This can be readily reparameterized into, for example, the frequency with which individuals are tested, compliance to the scheme, logistic delays and specificity of the employed test for infection.

II. Case isolation in heterogeneous populations

Assuming that the population is large, so that quantization effects become negligible, the trajectory of the epidemiological state subject to case isolation can be modeled as in [4]:

$$\frac{\mathrm{d}}{\mathrm{d}t}\begin{bmatrix} S \\ I \\ R \end{bmatrix} = \begin{bmatrix} -1 \\ 1 \\ 0 \end{bmatrix} \beta S(I-Q) + \begin{bmatrix} 0 \\ -1 \\ 1 \end{bmatrix} \gamma I, \quad S+I+R=1. \tag{1}$$

This model, which we will term *homogeneous* because of the uniform contact rates across the entire population, is a slight variant of the traditional SIR model of [6]. Here, as usual, S, I and R denote the proportions of the population that are susceptible, infectious, and removed and, as throughout, we have dropped the time-dependence in the variables to simplify notation when possible. The transitions between the states are governed by two rates that model the effect of disease spread and recovery, with mixing and recovery parameters β and γ, respectively. Note in particular that the mixing rate has been adjusted to account for the effect of isolating infectious individuals. More specifically,

$$Q(t) = \alpha e^{-\gamma T_{\text{delay}}} I(t - T_{\text{delay}}) \tag{2}$$

denotes the proportion of the population that is both infectious and isolated, subject to a time delay T_{delay} after infection. The rate that describes the spread of the disease has been modified so that the spread is only driven by interactions between the remaining infectious population and the susceptible population (the $\beta S(I-Q)$ term).

This captures to a first approximation the two most important features of a case isolation scheme, namely, how quickly infectious individuals are identified and isolated (T_{delay}), and what proportion of cases are found (α). However, the homogeneously interacting population is clearly a simplification. In reality, the interactions that may lead to infection are much more complex and hard to model. For example, you interact more frequently with people at your workplace than with people from a remote country. There is also a time-varying aspect. For instance, if your workplace issues a work-from-home guideline to reduce disease transmission, your rate of interaction with your coworkers will typically drop.

Numerous works have been dedicated to modeling the associated contact network dynamics, with [7], [8] and survey [9] constituting representative examples. The validity of such network models is hard to verify, and the time-varying aspects further increase the uncertainty surrounding their accuracy. We therefore delimit ourselves to a simple but important question: how does the introduction of interaction heterogeneity alter the requirements on our case isolation scheme (2), expressed in terms of the isolation proportion parameter α and associated time delay T_{delay}?

A. Heterogeneous population model

To account for contact rate heterogeneity, early models of infectious diseases (particularly STDs) [10], [11] incorporated a distribution of contact rates N_k/N defined as the proportion of the population of size N, who on average have k contacts per time unit (and in all other regards are homogeneous). It is assumed that a contact between a susceptible and infectious individual transmits an infection at a rate ρ. Using the formulation of [12], the disease dynamics for each partition $k = 0, 1, \ldots, n$ becomes

$$\frac{\mathrm{d}}{\mathrm{d}t}\begin{bmatrix} X_k \\ Y_k \end{bmatrix} = \begin{bmatrix} -k\lambda & 0 \\ k\lambda & -\gamma \end{bmatrix} \begin{bmatrix} X_k \\ Y_k \end{bmatrix}, \tag{3}$$

where X_k and Y_k denote, respectively, the number of susceptible and infectious individuals in each partition. This generalizes the standard SIR model for the homogeneous through the variable

$$\lambda = \rho \frac{\sum_{k=1}^{n} kY_k}{\sum_{k=1}^{n} kN_k}, \tag{4}$$

which is the rate at which infection is acquired from any one randomly chosen contact per time unit—now more likely to come from the partition with higher contact rates.

Remark 1 (Retrieving the homogeneous SIR model): When all individuals have k contacts per time unit, the rate of acquiring an infection from a randomly chosen contact in (4) simplifies to $\lambda = \rho Y/N = \rho I$. The disease dynamics (3) recover the traditional SIR model of [6] with mixing parameter $\beta = \rho k$ when divided by N. That is,

$$\frac{\mathrm{d}}{\mathrm{d}t}\begin{bmatrix} S \\ I \end{bmatrix} = \begin{bmatrix} -\beta I & 0 \\ \beta I & -\gamma \end{bmatrix} \begin{bmatrix} S \\ I \end{bmatrix}, \quad R = 1 - I - S, \tag{5}$$

where $S = X/N$, $I = Y/N$ (this is equivalent to (1) with $Q \equiv 0$).

B. Case isolation in a heterogeneous population

In arguably the simplest generalization of the case isolation scheme (2) to the heterogeneous population model (3), the number of individuals that are both isolated and infectious individuals in partition k is equal to some common proportion $0 \leq \alpha \leq 1$ of the infectious individuals Y_k, T_{delay} days in the past. This corresponds to a uniform identification and isolation scheme, independent of an individuals' number of contacts. Furthermore, it is assumed the partition size N_k is constant: isolated cases do not leave partition k, but are simply excluded from transmitting the disease. The number of infectious individuals in partition k then satisfies

$$Y_k(t) - Q_k(t), \quad Q_k(t) = \alpha e^{-\gamma T_{\text{delay}}} Y_k(t - T_{\text{delay}}), \tag{6}$$

and the rate at which an infection is acquired from any one randomly chosen contact becomes

$$\xi(t) = \rho \sum_i i(Y_i(t) - Q_i(t)) / \sum_k k N_k. \tag{7}$$

As a consequence of (7), the disease dynamics in each partition are described by the n delayed differential equations:

$$\frac{\mathrm{d}}{\mathrm{d}t}\begin{bmatrix} Y_1 \\ Y_2 \\ \vdots \\ Y_n \end{bmatrix} = \frac{\rho}{\sum_k N_k} \begin{bmatrix} X_1 \cdot 1 \\ X_2 \cdot 2 \\ \vdots \\ X_n \cdot n \end{bmatrix} \begin{bmatrix} 1 \\ 2 \\ \vdots \\ n \end{bmatrix}^\top \begin{bmatrix} Y_1 - Q_1 \\ Y_2 - Q_2 \\ \vdots \\ Y_n - Q_n \end{bmatrix} - \gamma \mathbf{I}_n \begin{bmatrix} Y_1 \\ Y_2 \\ \vdots \\ Y_n \end{bmatrix}. \tag{8}$$

About the all-susceptible equilibrium ($X_k = N_k$ for all k), the dynamics of the *total* number of infectious individuals in the heterogeneous population, $Y = \sum_k Y_k$, reads as

$$\frac{\mathrm{d}}{\mathrm{d}t} Y = \sum_k k N_k \xi - \gamma Y, \tag{9}$$

which can be written as a delayed differential equation in terms of λ. In turn, by differentiating (4) one obtains

$$\frac{d}{dt}\lambda = \frac{\rho}{\sum_k k N_k} \sum_i \left(i^2 N_i \xi \right) - \lambda \gamma Y. \tag{10}$$

All dynamics are described in terms of the number of individuals. By dividing by N, the population level disease dynamics with delayed case isolation are described by:

$$\begin{aligned} \frac{d}{dt}\begin{bmatrix} I \\ \lambda \end{bmatrix} &= \underbrace{\begin{bmatrix} -\gamma & \mu \\ 0 & \rho\left(\frac{\sigma^2}{\mu} + \mu\right) - \gamma \end{bmatrix}}_{\mathbf{A}_0} \begin{bmatrix} I \\ \lambda \end{bmatrix} \\ &+ \underbrace{\begin{bmatrix} 0 & -\mu\alpha e^{-\gamma T_{\text{delay}}} \\ 0 & -\rho\left(\frac{\sigma^2}{\mu} + \mu\right)\alpha e^{-\gamma T_{\text{delay}}} \end{bmatrix}}_{\mathbf{A}_1} \begin{bmatrix} I(t - T_{\text{delay}}) \\ \lambda(t - T_{\text{delay}}) \end{bmatrix}, \end{aligned} \tag{11}$$

where μ and σ represent the mean and standard deviation of the number of contacts per time unit. For a given delay T_{delay}, the system (11) is asymptotically stable if and only if all of the roots of

$$\det \underbrace{\begin{bmatrix} s + \gamma & -\mu(1 - \alpha e^{-(\gamma+s)T_{\text{delay}}}) \\ 0 & s - \rho\left(\frac{\sigma^2}{\mu} + \mu\right)(1 - \alpha e^{-(\gamma+s)T_{\text{delay}}}) + \gamma \end{bmatrix}}_{\mathbf{M} = s\mathbf{I}_2 - \mathbf{A}_0 - \mathbf{A}_1 e^{-sT_{\text{delay}}}} = 0, \tag{12}$$

are in the open left-half complex plane [13]. Because $\mathbf{M}$ is upper triangular, the roots of the characteristic equation (12) are $-\gamma$ and those of

$$f(s) = s - \rho\left(\frac{\sigma^2}{\mu} + \mu\right)(1 - \alpha \exp(-(\gamma + s)T_{\text{delay}})) + \gamma = 0. \tag{13}$$

Here, $f(s)$ is equivalent to the characteristic equation of the homogeneous case (1) with a scaled mixing parameter β linearized about $(S, I, R, Q) = (1, 0, 0, 0)$. This, together with our derivation above, leads to the following lemma.

Lemma 1: About the all-susceptible equilibrium $S_k = N_k$ for all $k = 1, \ldots, n$, the heterogeneous SIR model with delayed case isolation (6)–(8), and its population level disease dynamics (11), are asymptotically stable if and only if the linearization of the homogeneous model (1)–(2) about $(S, I, R, Q) = (1, 0, 0, 0)$ is asymptotically stable with mixing parameter $\beta = \rho\mu(c_v^2 + 1)$.

We will provide an explicit stability condition shortly, after reiterating the corresponding condition for the homogeneous case.

C. Comparing the homogeneous and heterogeneous population models

In the absence of case isolation, the equivalence of the stability condition between the heterogeneous and homogeneous SIR model, early in the epidemic, was first established in [10]. We now know the stability equivalence is also valid under the case isolation scheme with uniform identification and isolation of infectious individuals[1].

To compare the stability conditions of the heterogeneous and homogeneous model in terms of epidemiological variables, we briefly discuss the most common epidemiological measure (and source of confusion) for the spread of the disease: the reproduction number.

The reproduction number $\mathcal{R}$ describes the expected number of secondary infections caused by one primary infection. It holds that

$$\mathcal{R} \propto \underbrace{\left(\frac{\text{infection}}{\text{contact}}\right)}_{\rho} \cdot \underbrace{\left(\frac{\text{contact}}{\text{time}}\right)}_{c} \cdot \underbrace{\left(\frac{\text{time}}{\text{infection}}\right)}_{d},$$

where

- $\rho \in [0, 1]$: transmission rate given contact between a susceptible and infectious individual;
- $c \in \mathbb{R}_+$: average contact rate between susceptible and infectious individuals;
- $d \in \mathbb{R}_+$: average duration of infectiousness.

For the homogeneous population model (1) we have that $\beta = \rho c$ and $d = 1/\gamma$. It is also evident from (II-C) that the reproduction number reveals how *much* an epidemic grows, and not how *fast*. In order to quantify the latter,

[1]Having a common α in each partition is not necessary for the equivalence relation between the stability condition of the heterogeneous and homogeneous model to hold. For example, when α scales proportional to the number of contacts k in the partition ($\alpha_k = \alpha k/n$), the stability condition of the all susceptible equilibrium is equivalent to that of a common α that is scaled by $\langle k^3 \rangle / (n\sigma^2\mu^2)$, where $\langle k^3 \rangle$ is the third raw moment of the contact distribution.

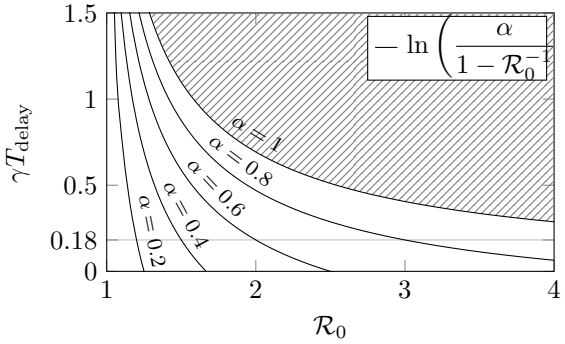

Fig. 1: Illustration of the stability boundary for the model (1)–(2). The model is stable if and only if $(\mathcal{R}_0, \gamma T_{\text{delay}})$ lies below the corresponding α curve. That is, at least a proportion α of persons becoming infectious on a particular day need to be isolated T_{delay} days later, given a natural recovery rate is γ days^{-1}.

the serial interval between infections is needed in addition. Yet, the reproduction number is more commonly used than the corresponding growth rate $r = \beta - \gamma$ among infectious disease epidemiologists, which is why we have chosen to use the former in our parametrization of fundamental limitations.

The basic reproduction number $\mathcal{R}_0$ is the reproduction in absence of a *considered* intervention. There is a common misconception that for a particular pathogen $\mathcal{R}_0$ is a universal constant (that can be looked up in the literature). Instead it depends on, among other time-varying parameters, the virulence of the pathogen and the societal structure under consideration. For instance, a particular virus would typically result in different $\mathcal{R}_0$'s in two countries, or in a city versus a village.

If an intervention is enacted, it is instead common to talk about the resulting effective reproduction number $\mathcal{R}_e$ (sometimes referred to as the time-varying reproduction number $\mathcal{R}_t$), and it really only makes sense to consider $\mathcal{R}_0$ in relation to a particular intervention: $\mathcal{R} = \mathcal{R}_0$ in absence of the intervention; $\mathcal{R} = \mathcal{R}_e$ if the intervention is enacted.

It was shown in [4] that for the case isolation scheme (2) applied to the model (1) the relation between $\mathcal{R}_0$ and $\mathcal{R}_e$ is given by

$$\mathcal{R}_e = \mathcal{R}_0 \left(1 - \alpha e^{-\gamma T_{\text{delay}}}\right), \quad \mathcal{R}_0 = \frac{\beta}{\gamma},$$

which is less than 1 if and only if [4, Theorem 2]

$$\gamma T_{\text{delay}} < \ln\left(\frac{\alpha}{1 - \mathcal{R}_0^{-1}}\right). \tag{14}$$

The specific trade-off between parameters and delay implied by (14) is shown in Fig. 1. This figure can be used to quickly assess the amount of delay that can be tolerated before instability, and hence exponential growth, occurs.

For example, with $\alpha = 0.8$, $\mathcal{R}_0 = 3$ and $\gamma = 0.1$, parameters chosen to be representative for SARS-CoV-2, the stability condition becomes

$$T_{\text{delay}}\gamma < 0.18, \quad \Longrightarrow \quad T_{\text{delay}} < 1.8 \text{ days}. \tag{15}$$

Clearly, short isolation times are essential when dealing with an infectious disease! We also see the importance of identifying a significant proportion of cases. When $\alpha < 2/3$ (that is, the scheme detects and isolates less than two thirds of the cases) exponential growth will occur even with $T_{\text{delay}} = 0$. We can use the equivalence relation in Lemma 1 to obtain the stability condition for the heterogeneous population model.

Proposition 2: Consider the population level disease dynamics with delayed case isolation linearized around the disease-free equilibrium, which is given for the heterogeneous model (11). The system dynamics are stable if and only if

$$T_{\text{delay}} < \frac{1}{\gamma} \ln\left(\frac{\alpha\beta h}{\beta h - \gamma}\right), \quad h = (c_v^2 + 1), \tag{16}$$

where $c_v = \sigma/\mu$ is the the coefficient of variation, or relative standard deviation.

Proof: The result follows from [4, Theorem 2] together with the stability equivalence relation established in Lemma 1. ∎

The stability condition in Proposition 2 implies that contact heterogeneity ($c_v > 0$) would *increase* the upper bound on T_{delay} if and only if the reproduction number of the corresponding homogeneous system ($\beta = \rho\mu$), in absence of control (2), fulfils $\mathcal{R}_0 < 1/h$. Since in the heterogeneous model $c_v > 0 \Leftrightarrow h > 1$, this requirement implies that heterogeneity would allow for a longer T_{delay} only if the uncontrolled system is *already stable* in the sense that $\mathcal{R}_0 < 1$. However, and of larger practical importance, the upper bound on the admissible T_{delay} will *decrease* when the heterogeneity (c_v) is increased whenever $\mathcal{R}_0 > 1$.

In the latter case, one may ask how large the coefficient of variation can be to allow for a positive delay and a stable equilibrium $(I, R, Q) = (0, 0, 0)$ of the linearized model with the scaled parameter β.

Corollary 3: For a basic reproduction number $\mathcal{R}_0 > 1$ of the corresponding homogeneously interacting population and $\alpha \in [0, 1)$, a positive delay is allowed in the heterogeneous population if and only if the coefficient of variance of the number of contacts satisfies

$$c_v^2 < \frac{1}{\mathcal{R}_0(1 - \alpha)} - 1. \tag{17}$$

Fig. 2 illustrates the effect of the coefficient of variance of the number of contacts on the upper bound of the delay (16), and the maximum allowed coefficient of variance c_v for several α that are isolated according to (6).

III. Numerical simulations

In this section, we study the role of network heterogeneity in the SIR model numerically in order to illustrate the stability condition (16).

A. Neighbors of infectious individuals

The phenomenon of the effective mixing parameter β increasing with increased heterogeneity (quantified by the coefficient of variation c_v) is also the answer to the question "Why your friends have more friends than you do", explained with mathematical insight in [14]. The intuition is that individuals with many contacts are more likely to get infected, and therefore the infectious proportion of the population

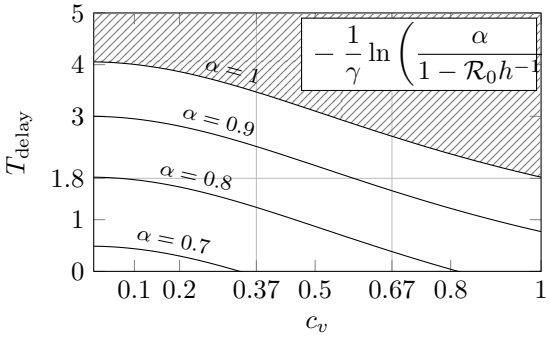

Fig. 2: Illustration of the stability boundary for the model (11) with $\mathcal{R}_0 = 3$ and $\gamma = 0.1$. The model is stable if and only if (c_v, T_{delay}) lies below the corresponding α curve. When $\alpha = 0.8$, the condition (17) reveals that the maximum coefficient of variation for which a positive isolation delay $T_{\text{delay}} > 0$ is allowed evaluates as $c_v \approx 0.82$ (where the $\alpha = 0.8$ intersects the horizontal axis). The vertical lines at $c_v = 0.37$ and $c_v = 0.67$ represent bounds on c_v for human infectious disease transmission networks from [8].

will comprise individuals who have more social contacts (higher degree) than those in the susceptible proportion of the population.

As with friendships, the contacts considered here are mutual, translating into an undirected network graph. Thus, the early spread of the disease is proportional to the mean number of contacts of a randomly chosen contact of an infectious individual (node), given by μh in (16) and illustrated in Fig. 3. Treating the network as homogeneous ($c_v = 0 \Leftrightarrow h = 1$) can therefore lead to an under-estimation of the reproduction number by disregarding the growth of the infectious sub-population, which is fueled by highly connected individuals, who are both more likely to acquire and spread the disease.

In Fig. 3 we have illustrated this effect through simulations of the early stage of 300 epidemics on different undirected random graphs representing a population. The nodes of each graph represent individuals; the edges contacts. For the example in Fig. 3, we chose to generate three different random graphs based on: 1) the configuration model, 2) Barabási-Albert and 3) Watts-Strogatz; for details on these random network models, see [15]. These random graphs were chosen to represent three fundamentally different networks. Each graph was generated with 10^6 nodes and an average degree $\mu = 4$.

The epidemics were each seeded by randomly assigning 10 infectious individuals on day one. This corresponds to $I = 10^{-5} \ll S = 1 - I$. The transmission probability, being the per-day probability that an edge between one infectious and one susceptible node leads to disease transmission, was set to $\rho = 0.2$. The recovery rate from (1) was set to $\gamma = 0.1$. Assuming independent interactions, the probability for a susceptible to become infectious the next day, given that it has m infectious contacts, is thus $1 - (1 - \rho)^m$.

In Fig. 3 (a)–(c), the results from the 300 epidemics simulations are shown. In particular, we see the average number of contacts of the infectious population throughout the early stages of the epidemic. From this figure we can clearly identify how the infectious individuals have a higher degree of contacts than the general population of the network. Furthermore, we can see that the average number of contacts of the infectious population early on tends towards a value equal to or smaller than the effective number of contacts $\mu + \sigma^2/\mu$. The same scaling defines the effective mixing parameter βh in the stability condition for a heterogeneous population (16).

To test if the effective number of contacts $\mu + \sigma^2/\mu$ actually gives an upper bound for the average number of contacts of the infectious population, it is also relevant to simulate the epidemic starting with average degree equal to $\mu + \sigma^2/\mu$. This can be done by choosing the initially infectious with a probability proportional to the degree of each node. The result of this simulation is shown in Fig. 3 (d)–(e). Here, we note that the average degree either remains constant or decreases for the three graphs. This indicates that the scaling factor $h = \sigma^2/\mu^2 + 1$ is conservative and represents the infectious population early on in an epidemic.

IV. Discussion

In Sec. II we generalized the case isolation scheme (2) of the homogeneous case isolation scheme to heterogeneous contact rate model and characterized how the stability boundary is moved if $\mathcal{R}_0$ of a homogeneous population is used in (14), when in fact the population is heterogeneous in the sense that the coefficient of variation of the contact network c_v is positive, while the mean degree remains unchanged.

Introducing heterogeneity in this way corresponds to multiplication of the mixing parameter β in (1) with the scaling factor $h = c_v^2 + 1$. Since β is directly proportional to $\mathcal{R}_0$, the heterogeneity can be interpreted as increasing the reproduction number by the corresponding factor. Note that the same shifting applies for a population partitioned based on heterogeneity of the infectiousness parameter ρ. This makes it possible to apply the same modeling to account for a variability in infectiousness across variants of the considered pathogen. Whether to multiply by the factor h before using $\mathcal{R}_0$ in the analysis comes down to how $\mathcal{R}_0$ was estimated from data. If it was estimated taking the heterogeneity into account it should not be adjusted, otherwise it should.

In the heterogeneous model (3) proposed in [12], the interaction between individuals with many and few contacts respectively are stochastic, and therefore do not correspond to a fixed (time-invariant) contact graph. For the case of a fixed contact graph, the stability bound (16) obtained for (3) would be conservative because of the assumption that the disease can spread to any contact of an infectious individual. In particular, an infectious individual cannot reinfect its own infector. Therefore, when considering epidemics on configurator model graphs, the shift of the epidemic threshold needs to be corrected by -1, resulting in $h = \sigma^2/\mu + \mu - 1$, as further discussed in [16]–[18].

Relatedly, clustering of the contact network result in the bound (16) becoming conservative. When many neighbors in the network are shared, (e.g. as in small-world networks) local clustering coefficients in the contact network are high

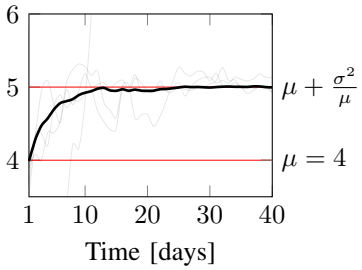

(a) Configuration model with Poisson distributed degrees and uniform initialization.

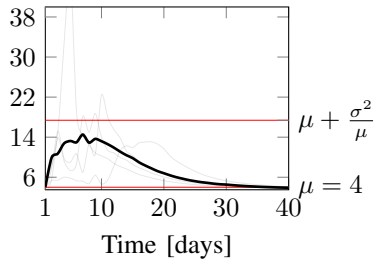

(b) Barabási–Albert graph and uniform initialization

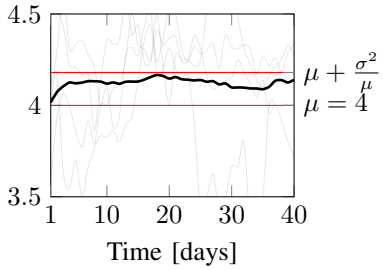

(c) Watts–Strogatz graph and uniform initialization.

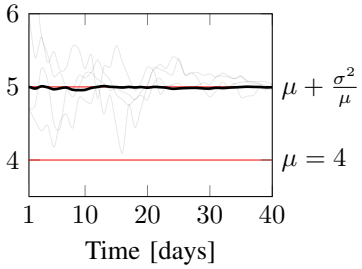

(d) Configuration model with Poisson distributed degrees and degree-based initialization.

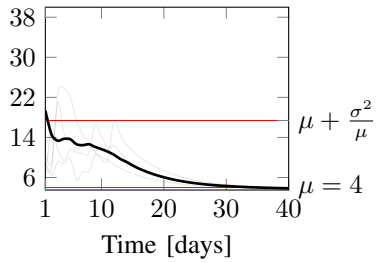

(e) Barabási–Albert degree-based initialization.

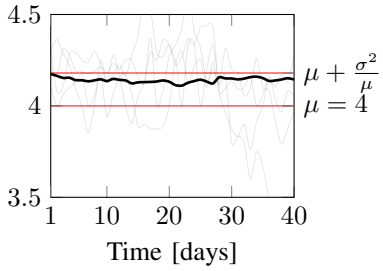

(f) Watts–Strogatz graph and degree-based initialization.

Fig. 3: 300 simulations were run for each scenario and then the average degree of the infectious population was calculated for each day. The simulation started with 10 infectious individuals. The dark line represent the average among all simulations. The effective number of contacts $\mu + \sigma^2/\mu$ and mean of degree distribution μ are marked in each sub-figure.

and voids the assumption that all neighbors of an infectious node are susceptible. To analytically quantify how local and global clustering effects affect the stability bound of the case isolation scheme, along the lines of [19], requires more complex network models. It falls outside the scope of this contribution, but is a worthwhile direction for future work.

V. Conclusion

Although obtaining detailed graph models of (the time-varying) human contact graphs relevant for infectious disease transmissions is generally not tractable, control theoretic analyses can provide qualitative, and to some extent quantitative criteria for the feasibility of strategies aimed at halting disease spread. This has been illustrated here by expressing stability conditions for case isolation schemes in homogeneous and heterogeneous populations, as functions of fundamental epidemiological parameters.

References

[1] D. Oliver, "Mistruths and misunderstandings about covid-19 death numbers," *British Medical Journal*, vol. 372, 2021.

[2] K. Soltesz, F. Gustafsson, T. Timpka, J. Jaldén, C. Jidling, A. Heimerson, T. Schön, A. Spreco, J. Ekberg, Ö. Dahlström, F. Bagge Carlson, A. Jöud, and B. Bernhardsson, "The effect of interventions on COVID-19," *Nature*, vol. 588, pp. E26–E28, 2020.

[3] F. Gustafsson and K. Soltesz, "NPI models explained and complained," *ISIF Perspectives on information fusion*, vol. 4, pp. 7–14, 2021.

[4] R. Pates, A. Ferragut, E. Pivo, P. You, F. Paganini, and E. Mallada, "Respect the unstable: delays and saturation in contact tracing for disease control," *Preprint*, 2021, available: https://mallada.ece.jhu.edu/pubs/2021-Preprint-PFPYPM.pdf.

[5] W. Topley and G. Wilson, "The spread of bacterial infection. the problem of herd-immunity," *The Journal of Hygiene*, vol. 21, no. 3, pp. 243–249, 1923.

[6] W. O. Kermack and A. G. McKendrick, "A contribution to the mathematical theory of epidemics," *Proceedings of the Royal Society of London A: mathematical, physical and engineering sciences*, vol. 115, no. 772, pp. 700–721, 1927.

[7] R. May, "Network structure and the biology of populations," *Trends in Ecology & Evolution*, vol. 21, no. 7, pp. 394–399, 2006.

[8] M. Salathé, M. Kazandjieva, J. Lee, P. Levis, M. Feldman, and J. Jones, "A high-resolution human contact network for infectious disease transmission," *Proceedings of the National Academy of Sciences*, vol. 107, no. 51, pp. 22 020–22 025, 2010.

[9] C. Nowzari, V. M. Preciado, and G. J. Pappas, "Analysis and control of epidemics: A survey of spreading processes on complex networks," *IEEE Control Systems Magazine*, vol. 36, no. 1, pp. 26–46, 2016.

[10] R. M. May and R. M. Anderson, "Transmission dynamics of HIV infection," *Nature*, vol. 326, no. 137, pp. 10–1038, 1987.

[11] R. May, S. Gupta, and A. McLean, "Infectious disease dynamics: what characterizes a successful invader?" *Philosophical Transactions of the Royal Society of London. Series B: Biological Sciences*, vol. 356, no. 1410, pp. 901–910, 2001.

[12] R. Anderson, G. Medley, R. May, and A. Johnson, "A preliminary study of the transmission dynamics of the human immunodeficiency virus (HIV), the causative agent of AIDS," *Mathematical Medicine and Biology: a Journal of the IMA*, vol. 3, no. 4, pp. 229–263, 1986.

[13] R. Sipahi, S.-I. Niculescu, C. T. Abdallah, W. Michiels, and K. Gu, "Stability and stabilization of systems with time delay," *IEEE Control Systems Magazine*, vol. 31, no. 1, pp. 38–65, 2011.

[14] S. Feld, "Why your friends have more friends than you do," *American Journal of Sociology*, vol. 96, no. 6, pp. 1464–1477, 1991.

[15] A.-L. Barabási, *Network Science*. Cambridge University Press, 2016.

[16] M. Newman, *Networks*. Oxford University Press, 2018.

[17] L. Meyers, "Contact network epidemiology: Bond percolation applied to infectious disease prediction and control," *Bulletin of the American Mathematical Society*, vol. 44, no. 1, pp. 63–86, 2007.

[18] I. Z. Kiss, J. C. Miller, P. L. Simon, *et al.*, *Mathematics of epidemics on networks*. Springer, 2017.

[19] P. Trapman, "On analytical approaches to epidemics on networks," *Theoretical population biology*, vol. 71, no. 2, pp. 160–173, 2007.